Nuclear structure of ^{109}Sb

T. Ishii,[1] A. Makishima,[2] M. Shibata,[1] M. Ogawa,[3] and M. Ishii[1]
[1]*Physics Division, Japan Atomic Energy Research Institute, Tokai-mura, Ibaraki-ken, Japan*
[2]*Center for Radioisotope Science, National Defense Medical College, Tokorozawa, Saitama-ken, Japan*
[3]*Department of Energy Sciences, Tokyo Institute of Technology, Midori-ku, Yokohama, Japan*
(Received 3 May 1993; revised manuscript received 6 December 1993)

This is the first report on nuclear structure of ^{109}Sb. Excited states up to $I^\pi = 27/2^+$ and $35/2^-$ have been established using the reaction ^{54}Fe(^{58}Ni,3p)^{109}Sb and in-beam techniques. According to the particle(hole)-core coupling scheme these excited states were classified into five bands: three are based on the $\pi d_{5/2}$, $\pi g_{7/2}$, and $\pi h_{11/2}$ states; the other two are the $\Delta I = 1$ collective bands built on the $17/2^+$ state at 2651 keV and the $23/2^-$ state at 4487 keV. The $11/2^+ \rightarrow 9/2^+$ transition in the $\pi g_{7/2}$ band possesses an $E2/M1$ mixing ratio $\delta > 0$, which suggests admixing of the $\pi g_{9/2}$ hole state. Positive mixing ratios observed in the collective bands indicate a prolate deformation due to the $(\pi g_{9/2})^{-1}$ core excitation. In the $\pi h_{11/2}$ band, $B(M1; 23/2^- \rightarrow 21/2^-)$ was measured to be 0.040(3) W.u. Furthermore the $27/2^- \rightarrow 25/2^-$ transition was too weak for a proton $M1$ transition. These transitions are retarded by the $\nu h_{11/2}$ configurations mixed in the involved states.

PACS number(s): 23.20.−g, 27.60.+j, 21.60.Cs

I. INTRODUCTION

Recently the study of high-spin states in light tin isotopes has made significant progress [1–6]. Not only single-particle levels were confirmed in the energy spectra but also collective levels were found at high excitation energies. Single-particle aspects can be ascribed to interacting valence neutrons around the inert core ^{100}Sn. As a matter of fact a shell model calculation [7] has succeeded in reproducing part of the energy spectrum of the yrast states and some others: those states having seniority $v \leq 6$ for the even isotopes ^{104,106,108}Sn and $v \leq 5$ for the odd ^{105,107}Sn. It also gave the reduced matrix elements: $\langle||M1||\rangle$ is in fairly good agreement with experiments but $\langle||E2||\rangle$ is too large for certain states. In ^{105,107}Sn [1,2,5] single-particle states fed from high-spin states indicate the weak coupling of an odd neutron and an even tin core. The calculated spectra support this observation. On the other hand the nuclear collectivity in tin isotopes is believed to involve the core excitation producing proton or neutron holes in the $g_{9/2}$ orbit. Even in a light tin isotope such as ^{108}Sn$\Delta I = 2$ decoupled bands have been found to appear at excitation energies above 6 MeV [4,6].

As well as the odd tin isotopes, nuclear structure of light, odd antimony isotopes may be described in terms of the particle(hole)-core coupling scheme. How an odd proton is coupled to an even tin core is an interesting subject for studying the p-n residual interaction. To date high-spin states have been observed in ^{113,117}Sb by in-beam techniques [8,9]. Energy spectra peculiar to the single closed shell and $\Delta I = 1, 2$ bands were revealed there. However, excessive neutrons complicate the nuclear structure of these nuclei and so make it difficult to study the detailed configurations. Therefore, the lighter isotopes are much better candidates for investigating this coupling scheme.

This is a motive of the present study, the first on nuclear structure of ^{109}Sb. An attempt is made here to assign the configurations to the excited states by comparison of transition properties between ^{109}Sb and ^{105}In. Furthermore, the magnitude of nuclear deformation is estimated for the collective states by an approximate method.

II. EXPERIMENTS

The present experiments all relied on a charged-particle multiplicity filter, Si box, for selection of the reaction channels producing antimony isotopes; for details of the Si box, see Refs. [10,11]. These include experiments on γ-γ coincidences, the γ-ray angular distribution, the γ-ray linear polarization, and the lifetime of excited states.

High-spin states in ^{109}Sb were populated by using the reaction ^{54}Fe(^{58}Ni,3p)^{109}Sb at a bombarding energy of 225 MeV. The target was a foil of ^{54}Fe, 98% enriched and 2.1 mg/cm^2; the foil was backed with an evaporated gold layer, 10.3 mg/cm^2. Gamma-gamma coincidences were recorded event by event using six Ge detectors; four of them were placed in the horizontal reaction plane and the others below the target in the vertical reaction plane; these were located 10 cm from the target, at angles of $90° \pm 30°$ with respect to the direction of the beam. The coincidences were accumulated for 70 h and totaled 1.2×10^8. The γ-ray angular distribution was measured at angles of 21° to 105° in steps of 12° with respect to the direction of the beam. The γ-ray linear polarization was observed with a polarimeter consisting of a single germanium crystal, 70 mm in diameter and 15 mm thick. The linear polarimeter was located at a center-to-center distance of 10 cm below the target and its surface was put in two positions, in and perpendicular to the reaction

plane. The γ-ray intensities were thus measured in the respective positions to determine the ratios $N_{\parallel}/N_{\perp}$, the anisotropies of linear polarization.

The lifetimes of the excited states were measured by the recoil distance method. An ^{54}Fe foil of 96% enrichment and 0.8 mg/cm^2 thickness was used for the lifetime measurement. The stopper was the 7.9 mg/cm^2 copper foil with a 2.3 mg/cm^2 layer of gold evaporated on the front surface. The Si box was split into two halves, front and back parts, between which the target and stopper foils were set. The allowed recoil distance was 3 mm and the accuracy of the measured distances was limited to ± 0.05 mm by the flatness of the target foil. The stop and flight peaks of γ rays were observed at two angles of 18° and 145° to resolve accidentally overlapping peaks, if any.

III. RESULTS

Candidates of γ rays from ^{109}Sb were picked out from the singles spectrum with charged-particle multiplicity $M = 3$. To confirm their origin and the transition cascades, coincidence spectra were projected from the event record for the gates set on these γ rays. Thus 67 γ rays were identified with transitions in ^{109}Sb. Their energies are listed in Table I. There are several doublets which were resolved by γ-γ coincidences. In particular a doublet of 179.5 and 179.9 keV γ rays is strongly fed in deexcitation of ^{109}Sb.

Figure 1 illustrates a few coincidence spectra. Spectrum (a) with the gate set on the 320 keV γ peak indicates existence of a collective band. Also spectrum (b) with the gate set on the 318 keV γ peak demonstrates intraband transitions in another collective band. Spectrum (c) shows a linkage between the ground-state band and an odd-parity band.

The relative intensities of the γ rays from ^{109}Sb were determined from the singles spectrum taken at 57° where the Legendre polynomial $P_2(\cos\theta)$ nearly vanishes. For unresolved γ rays, their relative intensities were evaluated from the coincidence spectra. The angular distributions of γ rays and their associated coefficients A_2 and A_4 were deduced from the singles spectra observed at the angles mentioned above. For adjacent γ rays unresolved, the coefficients A_2 and A_4 were determined for their doublet. These properties of the transitions are summarized in Table I.

Figure 2 shows the ratios $N_{\parallel}/N_{\perp}$ of γ transitions in ^{109}Sb and known transitions in ^{105}In [12] and ^{108}Sn [4]. The sensitivity of the linear polarimeter was too low ($\lesssim 5\%$) to measure the polarization with great accuracy. For this reason no attempt was made to determine the magnitudes of linear polarization but the ratios themselves were used to discriminate between magnetic and electric transitions: $N_{\parallel}/N_{\perp} > 1$ or < 1 corresponds to a pure, magnetic or electric transition, respectively. It should be noted here that the dipole transitions observed in ^{109}Sb can be classified into four groups: $A_2 \simeq \pm 0.15$,

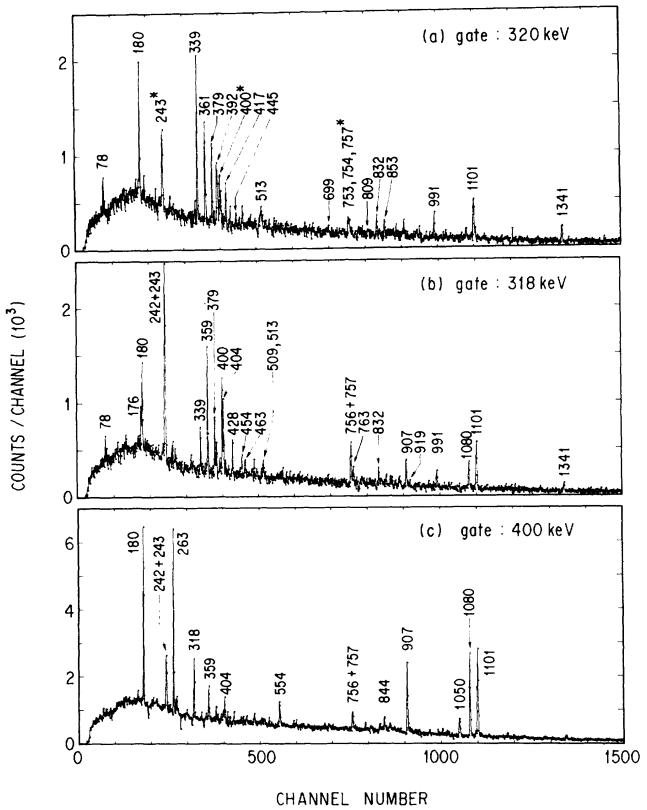

FIG. 1. Gamma-gamma coincidence spectra from ^{109}Sb. Spectra (a) and (b) demonstrate the transitions in the collective bands with even and odd parities, respectively. Spectrum (a) includes the asterisked (*) transitions in the odd-parity band since the 320 keV gate was contaminated by the 318 keV transition in that band. Spectrum (c) shows the linkage by the 400 keV $E1$ transition between the ground-state band and the $\pi h_{11/2}$ band.

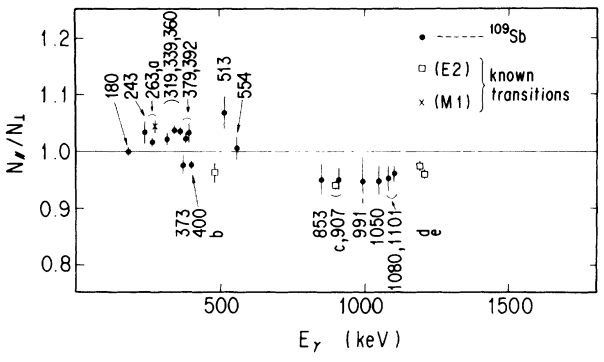

FIG. 2. Anisotropies $N_{\parallel}/N_{\perp}$ in linear polarization. The anisotropies for γ rays from ^{109}Sb are denoted by their energies in keV units and those for γ rays from other nuclei by alphabetical letters; **a** 272 keV ($19/2^+ \rightarrow 17/2^+$; ^{105}In). **b** 485 keV ($17/2^+ \rightarrow 13/2^+$; ^{105}In). **c** 906 keV ($4^+ \rightarrow 2^+$; ^{108}Sn). **d** 1195 keV ($8^+ \rightarrow 6^+$; ^{108}Sn). **e** 1206 keV ($2^+ \rightarrow 0^+$; ^{108}Sn). The anisotropy at 319 keV was evaluated for the doublet of the 318 and 320 keV γ rays. Also are given the anisotropies for the doublets: 180(180 + 180), 243(242 + 243), 339(339 + 339), and 360(359 + 361) keV.

TABLE I. The properties of γ-ray transitions in ^{109}Sb.

Energies (keV)	Relative intensities	Angular distributions A_2	A_4	Mixing ratios $\delta(Q/D)$	$I_i^\pi \rightarrow I_f^\pi$ (band No.)
77.8	18(5)	−0.21(3)	0.04(7)	∼ 0	$15/2^+ \rightarrow 13/2^+$(II)
168.6	4(1)[a]				$23/2^- \rightarrow 21/2^+$(III→I)
176.3	2(1)[a]				$21/2^- \rightarrow (19/2^-)$(V)
179.5	20(6)[b]	−0.27(3)[b]	0.02(7)[b]		$15/2^+ \rightarrow 13/2^+$(I)
179.9	44(13)[b]				$23/2^- \rightarrow 21/2^-$(III)
187.0	6(1)[a]				$19/2^- \rightarrow 17/2^+$(III→I)
241.5	12(2)[c]	−0.07(3)[c]	0.04(7)[c]	∼ +0.1	$23/2^- \rightarrow 21/2^-$(V)
243.3	16(3)[c]				$23/2^- \rightarrow 21/2^-$(V)
262.5	31(2)	−0.35(3)	0.04(7)	∼ −0.1	$21/2^- \rightarrow 19/2^-$(III)
268.6	3(1)	−0.19(8)	0.15(12)	∼ 0	$9/2^+ \rightarrow 7/2^+$(I→II)
318.4	23(6)[c]	−0.10(3)[c]	0.04(7)[c]	∼ +0.1	$25/2^- \rightarrow 23/2^-$(V)
320.1	17(5)[c]				$19/2^+ \rightarrow 17/2^+$(IV)
338.9	16(5)[b]	−0.10(3)[b]	0.04(7)[b]	∼ +0.1	$21/2^+ \rightarrow 19/2^+$(IV)
339.1	20(6)[b]				$13/2^+ \rightarrow 11/2^+$(II)
359.1	17(5)[c]	−0.10(3)[c]	0.06(7)[c]	∼ +0.1	$27/2^- \rightarrow 25/2^-$(V)
360.5	17(5)[c]				$23/2^+ \rightarrow 21/2^+$(IV)
373.1	17(2)	−0.21(3)	0.03(7)	∼ 0	$21/2^- \rightarrow 19/2^+$(III→I)
379.1	35(5)	−0.29(3)	0.04(7)	∼ −0.1	$17/2^+ \rightarrow 15/2^+$(I)
384.1	1(1)[a]				$21/2^+ \rightarrow 19/2^+$ (I)
392.4	15(3)	−0.14(5)	0.14(9)	∼ +0.1	$25/2^+ \rightarrow 23/2^+$(IV)
400.2	53(5)	−0.22(3)	0.05(7)	∼ 0	$11/2^- \rightarrow 9/2^+$(III→I)
403.6	12(2)	−0.08(5)	−0.01(9)	∼ +0.1	$29/2^- \rightarrow 27/2^-$(V)
416.7	4(1)[b]	−0.12(3)[b]	0.07(7)[b]	∼ +0.1	$15/2^+ \rightarrow 11/2^+$(II)
416.9	10(3)[b]				$27/2^+ \rightarrow 25/2^+$(IV)
428.2	7(2)	−0.05(5)	0.03(9)	∼ +0.1	$31/2^- \rightarrow 29/2^-$(V)
444.5	3(1)[a]				$(29/2^+) \rightarrow 27/2^+$(IV)
454.4	5(2)[a]				$33/2^- \rightarrow 31/2^-$(V)
462.0	4(2)[a]				$(21/2^+) \rightarrow 19/2^+$(I)
463.3	3(1)[a]				$35/2^- \rightarrow 33/2^-$(V)
496.3	1(1)[a]				$27/2^- \rightarrow 25/2^-$(III)
488.6	4(2)[a]				$15/2^- \rightarrow 13/2^+$(III→I)
508.6	6(2)[a]				$9/2^+ \rightarrow 7/2^+$(II)
511.6	4(2)[a]				$33/2^- \rightarrow 31/2^-$(III)
513.4	15(5)	0.15(3)	0.04(7)	∼ +0.28	$11/2^+ \rightarrow 9/2^+$(II)
554.0	18(3)	−0.42(5)	0.04(9)	∼ −0.1	$25/2^- \rightarrow 23/2^-$(III)
658.8	3(1)[a]				$21/2^+ \rightarrow 17/2^+$(IV)
678.5	3(1)[a]				$27/2^- \rightarrow 23/2^-$(V)
699.4	5(2)[a]				$23/2^+ \rightarrow 19/2^+$(IV)
727.1	2(1)[a]				$19/2^+ \rightarrow 17/2^+$(I)
752.6	4(2)[a]				$25/2^+ \rightarrow 21/2^+$(IV)
753.6	4(2)[a]				$11/2^+ \rightarrow 9/2^+$(II→I)
756.0	7(3)[c]	−0.42(5)[c]	0.09(9)[c]	∼ −0.1	$21/2^- \rightarrow 19/2^-$(V→III)
757.4	7(3)[c]				$21/2^- \rightarrow 19/2^-$(V→III)
763.0	5(2)[a]				$29/2^- \rightarrow 25/2^-$(V)
809.4	5(2)[a]				$27/2^+ \rightarrow 23/2^+$(IV)
832.1	4(2)[b]	−0.34(5)[b]	0.02(9)[b]	∼ −0.1	$31/2^- \rightarrow 27/2^-$(V)
832.2	18(4)[b]				$7/2^+ \rightarrow 5/2^+$(II→I)
837.3	7(2)	−0.18(8)	+0.16(12)	∼ 0	$19/2^- \rightarrow 17/2^+$(III→I)
843.7	13(2)	0.23(8)	0.09(12)		$31/2^- \rightarrow 27/2^-$(III)
847.5	5(2)[a]				$33/2^- \rightarrow 29/2^-$(III)
852.9	20(2)	0.26(5)	−0.02(9)		$13/2^+ \rightarrow 9/2^+$(II)
882.4	3(1)[a]				$33/2^- \rightarrow 29/2^-$(V)
907.4	39(8)[d]	0.31(5)[d]	−0.16(9)[d]		$19/2^- \rightarrow 15/2^-$(III)
918.6	3(1)[a]				$35/2^- \rightarrow 31/2^-$(V)
991.4	30(6)	0.29(3)	−0.10(7)		$13/2^+ \rightarrow 9/2^+$(I)
1003.8	6(2)	0.28(8)	0.12(12)		$29/2^- \rightarrow 25/2^-$(III)
1015.7	4(2)[a]				$(35/2^-) \rightarrow 31/2^-$(III)
1022.6	5(2)[a]				$11/2^+ \rightarrow 7/2^+$(II)

TABLE I. *(Continued).*

Energies (keV)	Relative intensities	Angular distributions A_2	A_4	Mixing ratios $\delta(Q/D)$	$I_i^\pi \rightarrow I_f^\pi$ (band No.)
1029.4	2(1)[a]				$17/2^+ \rightarrow 15/2^+$(I)
1050.0	26(4)	0.35(3)	−0.18(7)		$27/2^- \rightarrow 23/2^-$(III)
1079.7	46(3)	0.29(2)	−0.06(4)		$15/2^- \rightarrow 11/2^-$(III)
1093.3	16(3)	0.11(8)	−0.01(12)		$13/2^+ \rightarrow 9/2^+$(II→I)
1100.7	100	0.27(2)	−0.08(4)		$9/2^+ \rightarrow 5/2^+$(I)
1105.6	30(3)	0.30(3)	−0.21(7)		$19/2^+ \rightarrow 15/2^+$(I)
1111.3	6(3)	0.25(8)	−0.25(12)		$21/2^+ \rightarrow 17/2^+$(I)
1208.8	6(3)[a]				$17/2^+ \rightarrow 13/2^+$(I)
1341.1	29(9)[d]	0.25(8)[d]	−0.20(12)[d]		$9/2^+ \rightarrow 5/2^+$(II→I)

[a]Unresolved γ peaks in the singles spectrum with $M = 3$; the intensity of the γ ray from ^{109}Sb was evaluated from the γ-γ coincidences.

[b]A doublet of γ rays from ^{109}Sb; their intensities were evaluated from the γ-γ coincidence spectra and their angular distribution coefficients A_2 and A_4 were determined for the doublet.

[c]A doublet of γ rays from ^{109}Sb: their intensities were obtained from the singles spectrum with $M = 3$ but their angular distribution coefficients A_2 and A_4 were determined for the doublet.

[d]γ peaks including impurities; the 907 keV peak was contaminatd by the 906 keV γ ray from ^{108}Sn and the 1341 keV peak by the 1342 keV γ ray from ^{105}In; their intensities were obtained by subtracting the estimated intensities of the contaminants.

-0.1, -0.2, and -0.35. The group with $A_2 \simeq -0.2$ comprises rather pure transitions; they are the 78 and 269 keV $M1$ transitions and the 373 and 400 keV $E1$ transitions. The others include $M1/E2$ mixed transitions. As will be discussed later, the mixing ratios of these transitions give information about the nuclear configurations. In particular the 513 keV γ ray with $A_2 \simeq +0.15$ provides evidence for the core excitation $(\pi g_{9/2})^{-1}$.

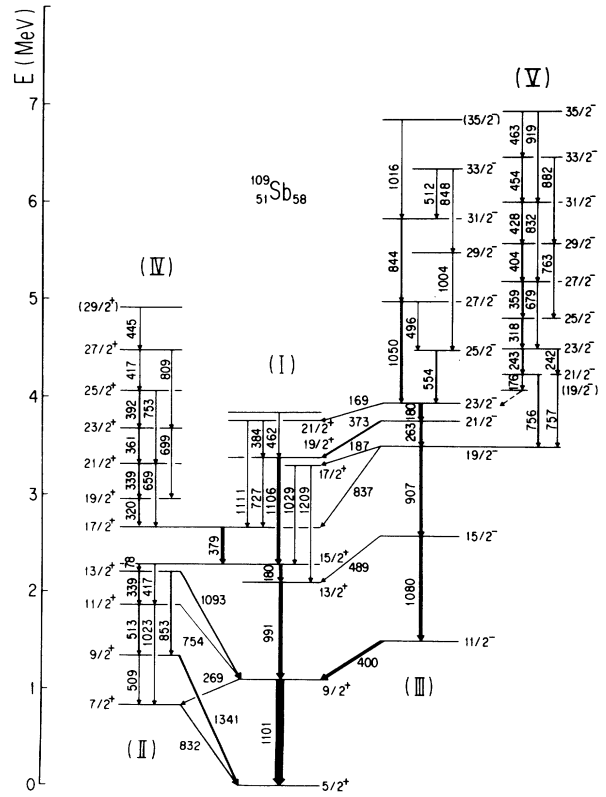

FIG. 3. A level scheme of ^{109}Sb. Excited states are classified into five bands according to the particle(hole)-core coupling scheme: three are based on the $\pi d_{5/2}$, $\pi g_{7/2}$, and $\pi h_{11/2}$ states and the other two are rotationally aligned collective bands.

The present study thus brought a level scheme of ^{109}Sb shown in Fig. 3. The transition cascades were placed there so as to conform with the γ-γ coincidences and the intensity balance at levels. For the reason mentioned later, $I^\pi = 5/2^+$ was assigned to the ground state. Spin parities of the excited states were determined from the observed multipolarities and parity changes of the transitions. It was also assumed that a highly excited nucleus deexcites with the decrease of angular momentum by emission of γ rays. In this work no transitions were observed from the $(19/2_2^-)$ state to the low-lying states. The γ-ray detection without Compton suppression must have missed such weak transitions. In Fig. 3 the excited states are classified into bands (I)–(V).

The lifetime of the $23/2^-$ state was measured by the recoil distance method. Figure 4 illustrates the decay curves for the 180 keV doublet, the 263 keV γ ray and the 379 keV γ ray. The doublet consists of the 179.9 keV transition from the $23/2^-$ state and the 179.5 keV transition from the $15/2^+$ state. The 263 keV transition succeeds the 179.9 keV transition. With $B(M1) \simeq 0.3$ W.u. obtained for the $19/2^+ \rightarrow 17/2^+$ transition in ^{105}In [12], the half-life of the $21/2^-$ state can be estimated to be a few ps. On the other hand the 1050 and 554 keV transitions feed the $23/2^-$ state within $T_{1/2} = 6$ ps. Thus the half-life of the decay curve for the 263 keV gives the half-life of the $23/2^-$ state: $T_{1/2}(23/2^-) = 84(7)$ ps.

The $15/2^+$ state is fed mainly by the 379 keV and 1106 keV transitions; $I_\gamma(379) = 35\%$, $I_\gamma(1106) = 30\%$. As seen from Fig. 4, the decay curve for the 379 keV transition is composed of a fast component ($T_{1/2} \lesssim 6$ ps) and a slow component from the $23/2^-$ state; the feeding ratio is about 2 to 1. A trace of the fast component was yet discerned in the decay curves for the 78 and 992 keV transitions but not for the 180 keV doublet. A numeri-

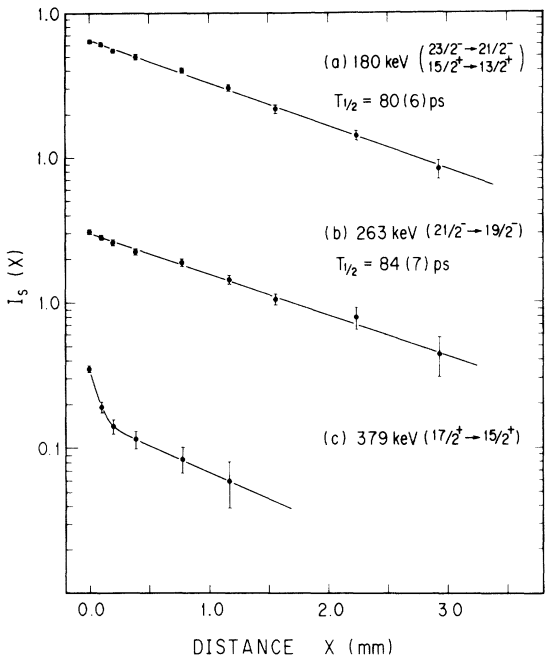

FIG. 4. The decay curves for (a) the 180 keV doublet, (b) the 263 keV γ ray, and (c) the 379 keV γ ray. The decay curves for γ rays were measured by the recoil distance method. The intensities of the stop peaks were measured relatively to that of the 254 keV γ ray from ^{108}Sn with a half-life of 7.3 ns. A recoil distance of 1 mm is equivalent to 79 ps. These three curves are substantially ruled by the lifetime of the $23/2^-$ state.

cal simulation for these observations gave the lower and upper bounds to the half-life of the $15/2^+$ state: 10 ps $\lesssim T_{1/2}(15/2^+) \lesssim$ 30 ps.

IV. DISCUSSION

A. The ground-state band

Neutrons in the orbits $\nu d_{5/2}, \nu g_{7/2}$, and $\nu h_{11/2}$ are involved in low excitation of light tin isotopes. According to the weak coupling model, low lying excited states in ^{107}Sn were classified into three bands based on these orbits [5]. Thus the proton analogues $\pi d_{5/2}$, $\pi g_{7/2}$, and $\pi h_{11/2}$ can be considered to play a similar role in ^{109}Sb. Since $\pi d_{5/2}$ has the lowest single-particle energy among the three, $I^\pi = 5/2^+$ is assigned to the ground state of ^{109}Sb. The experimental results agree with this assignment: the $7/2^+$ ground state could hardly account for the linkage by the observed $E1$ transitions between the ground-state band and the odd-parity band, band (III). Band (I) bears a close resemblance in level structure to the ground-state band in ^{107}Sn; the transition cascades from the $15/2^+$ to $13/2^+$ to $9/2^+$ to $5/2^+$ state are strongly populated there. This suggests that as well as in the $\nu d_{5/2}$ band of ^{107}Sn the multiplets: $\pi d_{5/2} \otimes \{^{108}\mathrm{Sn}\}_{0^+,2^+,4^+,6^+}$ split rather narrow. A shell model calculation for ^{107}Sn [7] shows that the $7/2_2^+$ and $11/2_2^+$ states are located in the vicinity of the $9/2^+$ and $13/2^+$ states, respectively. Band (I) is thus featured by the configurations: $\pi d_{5/2} \otimes \{^{108}\mathrm{Sn}\}_{0^+,2^+,4^+,\ldots}$. The $15/2^+$ and $17/2_1^+$ states belong to the multiplet $\pi d_{5/2} \otimes \{6^+\}$ and the $17/2_2^+$,$19/2^+$,and $21/2^+$ states to the $\pi d_{5/2} \otimes \{8^+\}$.

B. The $\pi g_{7/2}$ band and the $\pi g_{9/2}$ hole states

The $7/2^+$ state appears at an excitation energy of 832 keV. At first sight it might be taken as a member state of the multiplet $\pi d_{5/2} \otimes \{2^+\}$. However, the $9/2^+ \rightarrow 7/2^+$ interband transition is too weak for an intramultiplet transition. Its intensity is about $\frac{1}{30}$ the evaluated value from the branching ratio between the $E2$ and $M1$ transitions observed in ^{105}In. Thus the $7/2^+$ state is identified with the $\pi g_{7/2}$ state.

The $9/2^+$ and $11/2^+$ states of band (II) belong to the $\pi g_{7/2} \otimes \{2^+\}$ multiplet. However, they are far from the members of the pure multiplet. The $11/2^+ \rightarrow 9/2^+$ transition possesses an angular distribution coefficient $A_2 = 0.15$ and a linear polarization $P < 0$. From the plots of A_2 and P against $Q = \delta^2/(1+\delta^2)$ [13], the $E2/M1$ mixing ratio δ is evaluated to be $+0.28$. If the transition concerned were a pure intramultiplet transition, it would follow that $\langle||E2||\rangle < 0$ and $\langle||M1||\rangle > 0$, leading to $\delta < 0$. This is because core ^{108}Sn in a low-spin state is slightly deformed oblate and the $g_{7/2}$ proton has a positive g factor. So some configurations with $Q_0 > 0$ must be mixed in these states so as to give rise to a positive mixing ratio $\delta > 0$. Since the 9/2[404] Nilsson level appears at low excitation energies in $^{113-117}$Sb [14], the $\pi g_{9/2}$ hole states are likely to be admixed: $(\pi d_{5/2})_j^2 \otimes [(\pi g_{9/2})^{-1}\{^{108}\mathrm{Sn}\}_{0^+,2^+,4^+,\ldots}]$, where the two protons $(\pi d_{5/2})_j^2$ are taken to couple to $j = 0^+$ for economy of excitation energy.

The $M1/E2$ branching ratio at the $11/2^+$ state gives a crude estimate of the $\pi g_{9/2}$ hole amplitude in the $9/2^+$ state. First let us consider the transitions caused by the $\pi g_{7/2} \otimes \{2^+\}$ component of the $11/2^+$ state. The transition rates are given by $I(M1) = E^3B(M1)$ and $I(E2) = E^5B(E2)$. The branching ratio is thus written as follows: $I(M1)/I(E2) = 830E_1^3B(M1)/E_2^5B(E2)$, where γ-ray energy is measured in units of MeV and the reduced transition probabilities in the respective Weisskopf units. $B(E2)$ can be taken from the experimental value: $B(E2; 6^+ \rightarrow 4^+) = 2.3$ W.u. in ^{108}Sn [15]. $B(M1)$ for $\pi g_{7/2}$ can be estimated from that for $(\pi g_{9/2})^{-1}$ since $B(M1)$ is proportional to $(g_K - g_R)^2$; here g_K is the g factor of a particle or hole coupled to a core nucleus and g_R is that of the core. $B(M1)$ for $(\pi g_{9/2})^{-1}$ was measured to be 0.21 W.u. for the $19/2^+ \rightarrow 17/2^+$ transition in ^{107}In [12]. The 1023 keV $E2$ transition from the $11/2^+$ state has a relative intensity of 5% and the 513 keV $M1$ transition has 15%. Thus the intensity of the $M1$ transition caused by $\pi g_{7/2}$ is estimated to be: $I(M1) = 5\% \times 9[\Delta g(\pi g_{7/2})/\Delta g(\pi g_{9/2}\mathrm{hole})]^2$, where Δg is short for $(g_K - g_R)$. On the other hand $I(M1)$ for $(\pi g_{9/2})^{-1}$ and other admixtures

is at most 15%. Consequently the following result is obtained: $I(M1;\pi g_{9/2}\text{hole})/I(M1;\pi g_{7/2}) \simeq \frac{1}{3}[\Delta g(\pi g_{9/2}\text{hole})/\Delta g(\pi g_{7/2})]^2$. Here the multiplier of the $(\Delta g)^2$ ratio gives the square of the mixing ratio in amplitude.

C. A collective band with even parity

By contrast with band (II) of a single-particle nature, band (IV) shows a collective energy spectrum. This difference is likely to come from the $\pi g_{9/2}$ hole configurations. Band (IV) is confluent at the $17/2^+$ state into band (I) and then band (II) branches at the $15/2^+$ state from band (I). The $17/2^+ \rightarrow 15/2^+$ transition gives a clue for reasoning the involved configurations. It possesses $A_2 = -0.29$, $P < 0$ and so $\delta < 0$. A negative δ can be ascribed to an oblate deformation of the $\pi d_{5/2} \otimes \{6^+\}$ configurations. In this situation the following proton hole configurations can be mixed without changing the sign of δ and inducing either $E2$ or $M1$ transition: $(\pi d_{5/2})^2_{4^+}[(\pi g_{9/2})^{-1}\{^{108}\text{Sn}\}_{0^+}]$ in the $17/2^+$ state and $(\pi d_{5/2})^2_{0^+}[(\pi g_{9/2})^{-1}\{^{108}\text{Sn}\}_{4^+}]$ in the $15/2^+$ state. The former becomes the basis of rotationally aligned states and the latter is inherited by band (II).

Band (IV) may be considered to comprise the excited states with the rotationally aligned configurations: $(\pi d_{5/2})^2_{j=4^+}[(\pi g_{9/2})^{-1}\{^{108}\text{Sn}^*\}_{0^+,2^+,4^+,\ldots}]_{I'}$ with $I = I' + j$. Then the transition properties of the rotationally aligned nucleus are determined by a rotating, deformed core ^{108}Sn* with a $\pi g_{9/2}$ hole, strongly coupled together to (I', K). For example, since the deformed core with the hole has a prolate deformation and a positive g factor, the intraband $M1/E2$ mixed transitions there should show mixing ratios $\delta > 0$. This is the case for the $\Delta I = 1$ transitions observed in band (IV). Furthermore this simplification makes it feasible to evaluate the nuclear properties and to compare them with the existing data from other nuclei.

In Fig. 5, the moment of inertia is compared between band (IV) and the 9/2[404] band in ^{115}I [16]. The moment of inertia for the former band is plotted as a function of $(I - 4^+)$. The latter is typical of the 9/2[404] bands in the iodine isotopes $^{115-121}$I [16–18]. The fact that these plots are located close to each other means that the nucleus ^{109}Sb in band (IV) is deformed to almost the same extent as ^{115}I in the 9/2[404] band. For the 9/2[404] band Paul *et al.* [16] have estimated the nuclear deformation β to be larger than 0.25 from the branching ratios between intraband $E2$ and $M1$ transitions.

Their analysis was based on the semiclassical formalism of Dönau and Frauendorf [19]. Here the formula of $B(E2)$ and $B(M1)$ for an odd-mass deformed nucleus [20] are applied to estimate the intrinsic quadrupole moment Q_0; $B(E2; I_i \rightarrow I_f) = 5/16\pi C^2(I_i 2 I_f; K, 0, K)Q_0^2$ and $B(M1; I_i \rightarrow I_f) = 3/4\pi C^2(I_i 1 I_f; K, 0, K)K^2(g_K - g_R)^2$. Then the $B(E2)/B(M1)$ ratio between the intraband transitions is expressed as follows:

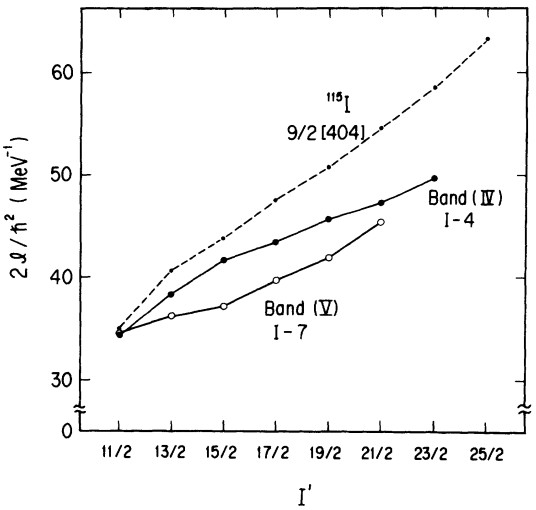

FIG. 5. Comparison of the moment of inertia between deformed bands. The moment of inertia is plotted against $(I - 4^+)$ for band (IV) and against $(I - 7^-)$ for band (V): $2\mathcal{I}/\hbar^2 = 2I'/[E(I') - E(I' - 1)]$, where $I' = I - j$. These plots are compared with that for the 9/2[404] band in ^{115}I.

$$\frac{B(E2; I \rightarrow I-2)}{B(M1; I \rightarrow I-1)} = \frac{5}{8}\frac{(I-1-K)(I-1+K)}{(I-1)(2I-1)K^2}\frac{Q_0^2}{(g_K - g_R)^2}$$

For the aligned configurations spin I should be replaced by $I' = I - j$. The g factor of the rotor with a $\pi g_{9/2}$ hole can be inferred from the g_R factors compiled by Prior *et al.* [21]; here g_R is taken to be 0.5. With g_Ω approximated by $g[(\pi g_{9/2})^{-1}] = 1.50$, g_K is evaluated to be 1.32. On the other hand the $B(E2)/B(M1)$ ratio was measured for the $21/2^+$ to $27/2^+$ states: it takes 0.085(25) $(eb/\mu_N)^2$ for $I = 21/2^+$ and increases with the spin to 0.15(3) $(eb/\mu_N)^2$ for $I = 27/2^+$. The above expression gives the Q_0 moment of 3.1 eb for the $27/2^+$ state, from which it follows that $\beta = 0.23$.

The present estimate includes uncertainties from the approximations but it is interesting to compare it with data from other nuclei. The odd antimony nuclei $^{115-121}$Sb have the static quadrupole moments around -0.4 eb in the ground state [22]. With a similar configuration as band (IV) except for $(\pi d_{5/2})^2_{4^+}$, ^{107}In in the $9/2^+$ ground state has a static quadrupole moment of 0.81eb [23] or an intrinsic moment of 1.5 eb. So it may be considered that ^{109}Sb in band (IV) is deformed to a considerable extent but not yet well-deformed.

D. Odd-parity states

Low-lying odd-parity states in ^{109}Sb are due to the $\pi h_{11/2}$ excitation. They are classified into bands (III) and (V) according as they are single-particlelike or collective.

The excitation energy of $\pi h_{11/2}$ is 1501 keV and is close to 1666 keV of $\nu h_{11/2}$ in ^{107}Sn [5]. The $11/2^-$, $15/2^-$,

$19/2^-$, and $21/2^-$ states in ^{109}Sb show a similar energy spectrum as in ^{107}Sn and so they must belong to the weak coupling multiplets: $\pi h_{11/2} \otimes \{^{108}\mathrm{Sn}\}_{0^+,2^+,4^+,6^+}$, respectively. However, it is somewhat anomalous that the $23/2^-$ state has a rather long lifetime. $B(M1; 23/2^- \rightarrow 21/2^-) = 0.040(3)$ W.u. is too small for a proton $M1$ transition. The $M1$ transition from the $27/2^-$ state affords substantial evidence for the configuration mixing of the $h_{11/2}$ neutron in the $23/2^-$ state: it possesses $\frac{1}{100}$ the intensity of the proton transition and the involved $|g_K - g_R|$ can be estimated to be about 0.1. Thus the configurations to admix are such that a pair of neutrons are broken and either one is excited in the $\nu h_{11/2}$ orbit. The $\Delta I = 1$ sequence of levels with $I^\pi = 25/2^-$ to $(35/2^-)$ must be due to the $\nu h_{11/2}$ excitation.

Band (V) can be considered to arise from the rotationally aligned configurations such as $(\pi d_{5/2}\pi h_{11/2})_{j=7^-}[(\pi g_{9/2})^{-1}\{^{108}\mathrm{Sn}^*\}_{0^+,2^+,4^+,\ldots}]_{I'}$ with $I = I' + j$. Spin-parity $j^\pi = 7^-$ is assigned to $(\pi d_{5/2}\pi h_{11/2})_j$. This is because the shell model calculation [7] shows that in ^{108}Sn the $3^-, 5^-$, and 7^- states are almost degenerate at the lowest excitation energy among the odd-parity states. Experimentally, as shown in Fig. 5, the moments of inertia for this band versus $(I - 7^-)$ behaves like that for the $9/2[404]$ band in ^{115}I. Furthermore the $M1/E2$ branching ratios show that band (V) has almost the same magnitude of the intrinsic quadrupole moment as band (IV).

The double excitation: $(\pi h_{11/2})^2$ may well take place at higher excitation energies. The probable configurations are $(\pi h_{11/2})^2_{j=10^+}[(\pi g_{9/2})^{-1}\{^{108}\mathrm{Sn}^*\}_{0^+,2^+,4^+,\ldots}]_{I'}$ and the excitation energy is estimated to be about 6 MeV for the band head state. So this band may intersect with band (IV) at 6 MeV or nearby, but the present study did not observe positive parity states beyond $I^\pi = (29/2^+)$.

V. CONCLUSION

High-spin states of ^{109}Sb were established up to $I^\pi = 27/2^+$ and $35/2^-$ using the reaction $^{54}\mathrm{Fe}(^{58}\mathrm{Ni},3p)^{109}\mathrm{Sb}$ and in-beam techniques. They were studied in terms of particle(hole)-core coupling scheme. Thus the excited states were classified into five bands: three were based on $\pi d_{5/2}$, $\pi g_{7/2}$, and $\pi h_{11/2}$; the other two were rotationally aligned collective bands. The electromagnetic properties of the $M1$ transitions in ^{109}Sb have revealed the following: The $(\pi g_{9/2})^{-1}$ configurations are admixed in the $9/2^+$ state and others of the $\pi g_{7/2}$ band. The $\nu h_{11/2}$ band is confluent at the $23/2^-$ state or nearby into the $\pi h_{11/2}$ band. The core nucleus ^{108}Sn involved in the collective bands is strongly coupled with a proton hole $(\pi g_{9/2})^{-1}$ and is deformed prolate: $\beta \sim 0.2$.

ACKNOWLEDGMENTS

The authors would like to thank Professor G. Momoki of the Nihon University and Professor K. Ogawa of the Chiba University for private communication about their shell model calculation. They also thank the JAERI tandem crew for supply of stable beams.

[1] R. Schubart, D. Alber, R. Alfier, C. Bach, D. B. Fossan, H. Grawe, H. Kluge, K. H. Maier, M. Schramm, M. Waring, and L. Wood, Z. Phys. A **340**, 109 (1991).

[2] T. Ishii, A. Makishima, K. Koganemaru, M. Nakajima, M. Ogawa, and M. Ishii, Report No. JAERI-M92-124, 1992, p. 143; M. Ogawa, K. Koganemaru, M. Nakajima, A. Makishima, T. Ishii, and M. Ishii, in *Proceedings of the 6th International Conference on Nuclei far from Stability and the 9th International Conference on Atomic Masses and Fundamental Constants,* Bernkastel-Kues, 1992, edited by R. Neugart and A. Wöhr (IOP, Bristol, 1992), p. 659.

[3] R. Schubart, H. Grawe, J. Heese, H. Kluge, K. H. Maier, M. Schramm, J. Grebosz, L. Käubler, H. Rotter, J. Kownacki, and D. Seweryniak, Z. Phys. A **343**, 123 (1992).

[4] F. Azaiez, S. Andriamonje, J. F. Chemin, M. Fidah, J. N. Scheurer, M. M. Aléonard, G. Bastin, J. P. Thibaud, F. Beck, G. Costa, J. F. Bruandet, and F. Liatard, Nucl. Phys. **A501**, 401 (1989).

[5] T. Ishii, A. Makishima, K. Koganemaru, Y. Saito, M. Ogawa, and M. Ishii, Z. Phys. A **347**, 41 (1993).

[6] R. Wadsworth, H. R. Andrews, R. M. Clark, D. B. Fossan, A. Galindo-Uribarri, J. R. Hughes, V. P. Janzen, D. R. LaFosse, S. M. Mullins, E. S. Paul, D. C. Radford, H. Schnare, P. Vaska, D. Ward, J. N. Wilson, and R. Wyss, Nucl. Phys. **A559**, 461 (1993).

[7] G. Momoki and K. Ogawa, private communication.

[8] V. P. Janzen, H. R. Andrews, B. Haas, D. C. Radford, D. Ward, A. Omar, D. Prévost, M. Sawicki, P. Unrau, J. C. Waddington, T. E. Drake, A. Galindo-Uribarri, and R. Wyss, Phys. Rev. Lett. **70**, 1065 (1993).

[9] D. R. LaFosse, D. B. Fossan, J. R. Hughes, Y. Liang, P. Vaska, M. P. Waring, and J.-y. Zhang, Phys. Rev. Lett. **69**, 1332 (1992).

[10] A. Makishima, Ph.D. thesis, Tokyo Institute of Technology, 1985; A. Makishima, M. Adachi, H. Taketani, and M. Ishii, Phys. Rev. C **34**, 576 (1986).

[11] M. Ishii, A. Makishima, M. Hoshi, and T. Ishii, in *Nuclei off the Line of Stability,* Washington, DC, 1986, edited by R. A. Meyer and D. S. Brenner (American Chemical Society, Washington, DC, 1986), p. 496.

[12] T. Ishii, A. Makishima, M. Nakajima, M. Ogawa, M. Ishii, Y. Saito, and S. Garnsomsart, Z. Phys. A **343**, 261 (1992).

[13] E. Der Mateosian and A. W. Sunyar, At. Data Nucl. Data Tables **13**, 391 (1974); **13**, 407 (1974).

[14] R. E. Shroy, A. K. Gaigalas, G. Schatz, and D. B. Fossan, Phys. Rev. C **19**, 1324 (1979).

[15] M. Hass, H. H. Bertschat, C. Broude, E. Dafni, F. D. Davidovsky, G. Goldring, and P. M. S. Lesser, Nucl. Phys. **A410**, 317 (1983).

[16] E. S. Paul, R. M. Clark, S. A. Forbes, D. B. Fossan, J. R. Hughes, D. R. LaFosse, Y. Liang, R. Ma, P. J. Nolan, P. H. Regan, P. Vaska, R. Wadsworth, and M. P. Waring, J. Phys. G **18**, 837 (1992).

[17] S. Juutinen, S. Törmänen, P. Ahonen, B. Cederwall, A. Johnson, B. Fant, R. Julin, S. Mitarai, J. Mukai, J. Nyberg, and A. Virtanen, Z. Phys. A **344**, 223 (1992).

[18] Y. Liang, D. B. Fossan, J. R. Hughes, D. R. LaFosse, T. Lauritsen, R. Ma, E. S. Paul, P. Vaska, M. P. Waring, and N. Xu, Phys. Rev. C **45**, 1041 (1992).
[19] F. Dönau and S. Frauendorf, in *Proceedings of the Conference on High Angular Momentum Properties of Nuclei,* Oak Ridge, 1982, edited by N. R. Johnson (Harwood Academic, New York, 1983), p. 143; F. Dönau, Nucl. Phys. **A471**, 469 (1987).
[20] A. Bohr and B. R. Mottelson, *Nuclear Structure* (Benjamin, New York, 1975), Vol. II, pp. 44–58.
[21] O. Prior, F. Boehm, and S. G. Nilsson, Nucl. Phys. **A110**, 257 (1968).
[22] P. Raghavan, At. Data Nucl. Data Tables **42**, 189 (1989).
[23] J. Eberz, U. Dinger, G. Huber, H. Lochmann, R. Menges, R. Neugart, R. Kirchner, O. Klepper, T. Kühl, D. Marx, G. Ulm, K. Wendt, and the ISOLDE Collaboration, Nucl. Phys. **A464**, 9 (1987).